Universidad del País Vasco
Euskal Herriko Unibertsitatea

ZTF-FCT
Zientzia eta Teknologia Fakultatea
Facultad de Ciencia y Tecnología

Gradu Amaierako Lana / Trabajo Fin de Grado
Fisikako Gradua / Grado en Física

Numerical simulation of the interference between two Bose-Einstein condensates

Egilea/Autor:
Ander Movilla
Zuzendariak/Directores:
Michele Modugno
Iñigo Luis Egusquiza

Leioa, 2016ko ekainaren 24a /Leioa, 24 de junio de 2016

Contents

Introduction

A Bose-Einstein condensate (BEC) is a macroscopic state of matter where, essentially, all atoms occupy the same quantum state and quantum phenomena become apparent. This state can only be achieved by systems of identical bosons, namely, integer spin particles that obey Bose statistics. Due to the intrinsically quantum nature of a BEC its mathematical description must be made by wave functions, just as for any other system governed by the laws of quantum mechanics.

BECs were first predicted by Albert Einstein in 1924 [1] following the work done by Satyendra Nath Bose on the statistics of photons, which are bosons as well. However, it was not until 1995 that the first BEC was realised experimentally. It was done using dilute gases of alkali atoms by the groups of Eric Cornell and Carl Wieman at the University of Colorado at Boulder with rubidium (^{87}Rb) [2] and shortly after by the group of Wolfgang Ketterle at MIT with sodium (^{23}Na) [3]. The three of them received the Nobel prize in physics in 2001 for this achievement.

A BEC in dilute atomic gases system differs from other states of matter in a number of respects, some of which I will outline here. First of all, the particle density at the center of the condensed atomic cloud is typically of $10^{13} - 10^{15} cm^{-3}$ which is nearly 6 orders of magnitude less than that of air at room temperature and atmospheric pressure. The temperature in these systems must be of the order of $10^{-5} K$, or even less, for it to show BEC (see Chapter 1 of Ref. [4]). In this kind of experiments the total number of particles is of the order of 10^5.

BECs are macroscopic quantum systems, a feature that makes them show quantum phenomena, for example, superfluidity, quantized vortices or interference. Their macroscopic size makes them a very interesting system, ideal to study such effects. In BECs the quantum probability distribution given by the wave function is, indeed, a matter distribution of the atoms that form the condensate, which enables a direct measurement of these quantum phenomena already mentioned, normally by optical means. Moreover, BECs are attractive experimentally because there are techniques to manipulate them using lasers or magnetic fields.

The main objective of this thesis is to study the interference between two Bose-Einstein condensates by means of numerical simulations. The present work is organised as follows: in Chapter 1 the basic theory of BEC in the mean field regime is presented (the Gross-Pitaevskii theory), in Chapter 2 it is sketched a method for solving numerically the Gross-Pitaevskii equation and in Chapter 3 the interference of two different freely expanding BECs is studied both analytically and numerically and is compared with the landmark experiment in Ref. [11]. Finally, the most important conclusions will be outlined. In the appendix we briefly review the methods that have been employed in the numerical solution of the Gross-Pitaevskii equation.

Chapter 1

Gross-Pitaevskii Theory

The aim of this chapter is to give an accurate mathematical description of Bose-Einstein Condensates (BECs) in order to be able to study interference phenomena between two BECs.

1.1 Order Parameter

We will start by considering a system of N identical bosons, each of them represented by a spatial coordinate $\mathbf{r}_i$. To simplify the present discussion we will assume that the system has no time dependence but this will not affect the result of our discussion. We will also, for the moment, consider that there is no interaction among the bosons. As stated before, the quantum properties of a BEC forces us to make their description in terms of wave functions. Therefore, the description of this system can be made in terms of a many body wave function of the form $\Psi_N(\mathbf{r}_1, \mathbf{r}_2, ...\mathbf{r}_N)$. As the system is composed of identical bosons this wave function has to be completely symmetric with respect to the interchange of any two spatial coordinates, $\mathbf{r}_i \leftrightarrow \mathbf{r}_j$.

The simplest way of writing, approximately, this many body wave function is as a product of single-particle states that fulfils the symmetry conditions. This is known as the Hartree-Fock ansatz, or, when applied to Bose-Einstein condensate systems, the Gross-Pitaevskii approximation. Later on, this simplification will prove to be useful at very low temperatures when trying to predict the behaviour of Bose-Einstein condensates in a variety of situations.

If the system is in thermal equilibrium, in the grand-canonical ensemble, it is described

by the Bose-Einstein distribution:

$$n_i = \frac{1}{e^{\beta(\varepsilon_i - \mu)} - 1}, \quad \beta = \frac{1}{k_B T} \tag{1.1}$$

where n_i is the number of bosons in a quantum state of energy ε_i and k_B is the Boltzmann constant. The Bose-Einstein distribution predicts a phase transition at a temperature T_c (critical temperature), below which there is a quantum state macroscopically occupied. According to equation (1.1), at $T = 0$ all the particles will be in the lowest single-particle state, so that the many body wave function becomes

$$\Psi_N(\mathbf{r}_1, \mathbf{r}_2, ...\mathbf{r}_N) = \prod_{i=1}^{N} \varphi_0(\mathbf{r}_i) \tag{1.2}$$

This wave function describes the ground state of the system, which corresponds to a Bose-Einstein condensate where all the particles are occupying the same quantum state.

This single-particle state, φ_0, will be referred from now on as the condensate wave function and the number of particles in it, N_0, the number of particles in the condensate. Taking into account the above considerations, we are in a position to define the order parameter of a BEC, which is realised in the state φ_0 occupied by N_0 particles. Then, the order parameter is

$$\psi(\mathbf{r}) \equiv \sqrt{N_0}\varphi_0(\mathbf{r}) \tag{1.3}$$

which is simply the single-particle wave function with a normalisation. This order parameter describes the behaviour of the condensate and, therefore, can be regarded as a macroscopic wave function of the condensate. In this approximation, also called the mean field approximation, quantum and thermal fluctuation are neglected for being small compared to the macroscopic occupation of the condensate. Then, in this notation we get the following expression for the density, n, of the condensate:

$$n(\mathbf{r}) = |\psi(\mathbf{r})|^2. \tag{1.4}$$

The order parameter can also be written in the following form

$$\psi(\mathbf{r}) = |\psi(\mathbf{r})|e^{iS(\mathbf{r})}. \tag{1.5}$$

Here the modulus determines the density of the condensate and $S(\mathbf{r})$ is a phase that will play an important role when studying the coherence properties of BEC. However, we have some freedom when fixing the value of this phase. One can always multiply the order parameter by $e^{i\phi}$ and the resulting order parameter will describe exactly the same state (see Chapter 2 in Ref. [8]). This is a consequence of the global gauge symmetry inherent in this description. I would like to emphasise that changing globally the phase by a factor has no physical meaning but local changes may alter physically relevant quantities such as the velocity of the condensate flow, that will be introduced in section 1.3.2. Yet, when a Bose system is below its critical temperature and BEC occurs, its phase ϕ becomes well defined [13]. It is therefore said to have spontaneously broken gauge symmetry.

1.2 Effective Interaction

Until now we have considered the case of noninteracting bosons but real condensates, like the ones used in experiments, do have interactions. In the following we will consider the effect of the interatomic interactions in a dilute gas at low temperatures, conditions fulfilled in BECs.

The interaction between two atoms in a dilute gas has only one relevant variable, namely, their relative coordinate $\mathbf{r}$. The interaction is described by an interatomic potential $V_{at}(|\mathbf{r}|)$, which only depends on the separation of the two atoms. However, at sufficiently low energies, the scattering of a particle by a potential does not depend on the shape of the potential but on a single parameter related with it, the scattering length a.

When dealing with this kind of problems it is common to perform a partial wave expansion in which each term of the expansion corresponds to a value of the angular momentum l and it is treated separately. Since we are considering the case of low energy it seems a reasonable assumption to restrict ourselves to s-wave scattering ($l = 0$) and neglect the rest of the terms. Therefore, the only parameter of the potential that really matters is the s-wave scattering length, a_s. For our case, ^{23}Na, the value taken by the s-wave scattering length is $a_s = 3$ nm.

The following is based on the discussion in section IV of Ref. [5] and uses the corresponding notations. Bearing in mind the above considerations the true interatomic potential, $V_{at}(|\mathbf{r}|)$, can be substituted by a pseudopotential of the form of a delta function in the origin. Then the effective interaction turn to be

$$V_{eff}(\mathbf{r}) = \frac{4\pi a_s \hbar^2}{m}\delta(\mathbf{r}). \tag{1.6}$$

This is equivalent to say that the mean interaction energy of the many body system is given by

$$\langle E_{int}\rangle = \frac{1}{2}\frac{4\pi a_s \hbar^2}{m}\sum_{ij}|\Psi(r_{ij}\to 0)|^2 \tag{1.7}$$

where Ψ is the many body wave function, $r_{ij} = |\mathbf{r}_i| - |\mathbf{r}_j|$ and $r_{ij} \to 0$ means that the separation between any two atoms of the condensate is very small compared the averaged distance between particles, $d \equiv v^{1/3} = (V/N)^{1/3}$, and the thermal wavelength, $\lambda_T = \sqrt{2\pi\hbar^2/(mk_BT)}$, but large compared to a_s. This can be understood as $|\Psi|^2$ averaged over a volume larger than a_s^3. The reason to do this is that a particle, in quantum mechanics, is not localised in a point of the space but it is "spread" over a distance comparable to its thermal wavelength. Therefore, the particle will experience an averaged effect of the potential.

For equation (1.7) to be valid several conditions need to be fulfilled. The first condition is to work at first order in a_s when evaluating $\langle E_{int}\rangle$. Next, as stated before, $l \neq 0$

scattering must be negligible. In addition, we require that $d \gg a_s$, which generally holds due to the diluteness hypothesis of the gas. Finally, $\lambda_T \gg a_s$ enables us to take only into account the averaged effect of the potential.

It will be useful in the following sections to put equation (1.7) in terms of the order parameter. In the Hartree-Fock approximation we can take the two particle wave function to be

$$\Psi(\mathbf{r}_i, \mathbf{r}_j) \simeq \phi(\mathbf{r}_i)\phi(\mathbf{r}_j) \tag{1.8}$$

that yields

$$\langle E_{int} \rangle_{ij} = \frac{4\pi\hbar^2 a_s}{m} \int |\varphi(\mathbf{r})|^4 d\mathbf{r} \tag{1.9}$$

as the mean interaction energy between any two atoms i and j. Adding the interaction between every pair of atoms in the condensate, and neglecting three particle interaction, we get

$$\langle E_{int} \rangle = \frac{1}{2} \frac{4\pi a_s \hbar^2}{m} \sum_{i,j} \int |\varphi(\mathbf{r})|^4 d\mathbf{r} = \frac{1}{2} \frac{4\pi a_s \hbar^2}{m} N(N-1) \int |\varphi(\mathbf{r})|^4 d\mathbf{r}. \tag{1.10}$$

Here and in equation (1.7) arises a 1/2 factor in order to count each interaction between a particle i and a particle j only once and not twice.

1.3 The Gross-Pitaevskii Equation

Until now, only a mathematical description of a typical BEC has been given but nothing has been said about how this system evolves with time. In this section we will derive an equation that governs the time dependence of the order parameter and, hence, the time dependence of the condensate. This section is based on the derivation given section V of Ref. [5].

Taking into account considerations of the two sections above, it is easy to find the expectation value of the energy as

$$\begin{aligned} \langle H \rangle &= \int \psi^* H \psi = \int \psi^*(\mathbf{r})(H_{kin} + H_{V_{pot}}(\mathbf{r}) + H_{int})\psi(\mathbf{r}) \\ &= N \int d\mathbf{r} \left\{ \frac{\hbar^2}{2m} |\nabla\varphi_0(\mathbf{r})|^2 + V_{ext}(\mathbf{r})|\varphi_0(\mathbf{r})|^2 \right\} + \frac{N(N-1)}{2} g \int d\mathbf{r} |\varphi_0(\mathbf{r})|^4 \end{aligned} \tag{1.11}$$

where

$$g \equiv \frac{4\pi\hbar^2 a_s}{m}. \tag{1.12}$$

Normally in BEC experiments the number of bosons, N, is of the order of 10^5, which enables us to make the approximation $N \simeq N - 1$. To obtain a dynamic equation from $\langle H \rangle$ it is necessary to minimise equation (1.11) with the constraint of the normalisation

of φ_0. The minimisation is expressed mathematically by the following adaptation of the Euler-Lagrange equations (see chapter 22 of Ref. [6])

$$\frac{\partial\langle H\rangle - \mu|\varphi_0(\mathbf{r})|^2}{\partial\varphi_0(\mathbf{r})} - \frac{d}{d\mathbf{r}}\frac{\partial\langle H\rangle - \mu|\varphi_0(\mathbf{r})|^2}{\partial\nabla\varphi_0(\mathbf{r})} = 0 \tag{1.13}$$

where μ is the Lagrange multiplier associated with the constraint (see equation (1.13))

$$\int |\varphi_0|^2 d\mathbf{r} = 1. \tag{1.14}$$

This yields

$$-\frac{\hbar^2}{2m}\nabla^2\varphi_0(\mathbf{r}) + V_{ext}(\mathbf{r})\varphi_0(\mathbf{r}) + Ng|\varphi_0(\mathbf{r})|^2\varphi_0(\mathbf{r}) = \mu\varphi_0(\mathbf{r}) \tag{1.15}$$

where the change $\mu = \mu/N$ has been made. Rewriting the previous equations in terms of the order parameter, that in this case is nothing more than normalising the wave function to N,

$$-\frac{\hbar^2}{2m}\nabla^2\psi(\mathbf{r}) + V_{ext}(\mathbf{r})\psi(\mathbf{r}) + g|\psi(\mathbf{r})|^2\psi(\mathbf{r}) = \mu\psi(\mathbf{r}) \tag{1.16}$$

which is the stationary Gross-Pitaevskii equation (GPE), derived independently by Gross and Pitaevskii in 1961. Now, we generalise this result to the time-dependent case in the following way

$$i\hbar\frac{\partial\psi(\mathbf{x},t)}{\partial t} = -\frac{\hbar^2}{2m}\nabla^2\psi(\mathbf{r},t) + V_{ext}(\mathbf{r})\psi(\mathbf{r},t) + g|\psi(\mathbf{r},t)|^2\psi(\mathbf{r},t) \tag{1.17}$$

where it has been supposed the following time-dependence of the order parameter

$$\psi(\mathbf{r},t) = \psi(\mathbf{r})e^{-i\mu t/\hbar}. \tag{1.18}$$

In the Gross-Pitaevskii equation μ, the chemical potential, is the variable that determines the time dependence of a BEC as the energy does in the systems that obey the Schrödinger equation. In the case of the GPE, the chemical potential is not equal to the total energy, E, due to the nonlinear term present in the equation. Indeed,

$$\mu = \frac{\partial E}{\partial N}. \tag{1.19}$$

This can be seen by multiplying equation 1.15 by $\varphi_0^*(\mathbf{r})$, integrating over the volume and comparing it with the value of $\langle H\rangle$ given in equation (1.11).

The time dependent GPE will be the main tool when studying the interference phenomena of two BECs. In order to do this is necessary to know how to solve it numerically, which is the objective of Chapter 2.

1.3.1 Functional derivation of the Gross-Pitaevskii Equation

An alternative way of deriving the GPE is taking as a starting point the energy functional of a BEC.

The energy functional can be constructed by comparison with $\langle H \rangle$ in equation (1.11). Therefore, in terms of the order parameter the energy functional takes the following form (see chapter 2 of Ref. [7])

$$E[\psi] = \int d\mathbf{r} \left\{ \frac{\hbar^2}{2m} |\nabla \psi(\mathbf{r})|^2 + V_{ext}(\mathbf{r}) |\psi(\mathbf{r})|^2 + \frac{gN}{2} |\psi(\mathbf{r})|^4 \right\} \tag{1.20}$$

where the three different terms in the functional represent different energies; kinetic energy for the first term, potential energy (due to the external potential) for the second one and the interaction energy for the third one.

By using the variational ansatz

$$i\hbar \frac{\partial \psi(\mathbf{r})}{\partial t} = \frac{\delta E}{\delta \psi^*} \tag{1.21}$$

we obtain again the GPE.

1.3.2 Hydrodynamic formulation of the Gross-Pitaevskii Equation

There is an alternative way of formulating the GPE in terms of two coupled equations that resemble those that appear in fluid mechanics.

To derive this equation we will consider another representation of the order parameter, namely,

$$\psi(\mathbf{r}, t) = \sqrt{n(\mathbf{r}, t)} e^{iS(\mathbf{r}, t)} \tag{1.22}$$

where $n(\mathbf{r}, t)$ represents the density of the condensate at the point $\mathbf{r}$ and time t. By substituting this version of the order parameter into the GPE and equating the real and imaginary parts separately we get the following pair of equations

$$\frac{\partial n}{\partial t} + \nabla(n\mathbf{v}) = 0 \tag{1.23}$$

$$m \frac{\partial \mathbf{v}}{\partial t} + \nabla \left\{ -\frac{\hbar^2}{2m} \frac{(\nabla^2 \sqrt{n})}{\sqrt{n}} + \frac{1}{2} m\mathbf{v}^2 + V_{ext} + gn \right\} = 0 \tag{1.24}$$

where $\mathbf{v}(\mathbf{r}, t)$ is the velocity of the condensate flow obtained from the phase $S(\mathbf{r}, t)$ in the following way

$$\mathbf{v}(\mathbf{r}, t) = \frac{\hbar}{m} \nabla S(\mathbf{r}, t). \tag{1.25}$$

Equation (1.23) is the continuity equation, that corresponds to the conservation of mass, and equation (1.24) is an analogous of the Euler equation for an ideal fluid. In this last equation the term

$$-\frac{\hbar^2}{2m} \frac{(\nabla^2 \sqrt{n})}{\sqrt{n}}$$

is called the quantum pressure term, which is a consequence of the Heisenberg uncertainty principle.

By substituting equation (1.25) into equation (1.24) we obtain an explicit equation for the evolution of the phase of the condensate, namely,

$$\hbar\frac{\partial}{\partial t}S + \left(\frac{1}{2}m\mathbf{v}^2 + V_{ext} + gn - \frac{\hbar^2}{2m}\frac{(\nabla^2\sqrt{n})}{\sqrt{n}}\right) = 0 \tag{1.26}$$

which will be useful later.

1.4 Thomas-Fermi Regime

The Thomas-Fermi (TF) regime or TF limit is characterised by a slowly varying density of the gas in space, which makes the quantum pressure term negligible [8]. Therefore, in this limit the interaction term dominates over the kinetic term of the GPE, enabling us to write this equation in a very simple form

$$V_{ext}(\mathbf{r})\psi(\mathbf{r}) + g|\psi(\mathbf{r})|^2\psi(\mathbf{r}) = \mu\psi(\mathbf{r}) \tag{1.27}$$

whose solution is

$$\psi(\mathbf{r}) = \sqrt{\frac{\mu - V_{ext}(\mathbf{r})}{g}} \quad \text{where} \quad \mu \geq V_{ext} \tag{1.28}$$

$$\psi(\mathbf{r}) = 0 \qquad\qquad \text{elsewhere.} \tag{1.29}$$

In experimental setups it is usual to use harmonic potentials as external potential. As this case will be useful in the future, we will develop the solution given above for this kind of potentials.

The solution takes the form

$$\psi(\mathbf{r}) = \sqrt{\frac{\mu}{g} - \sum_i \frac{m\omega_i^2}{2g}x_i^2} \tag{1.30}$$

which is, again, only valid when the argument of the square root is positive or zero, the wave function is vanishing elsewhere. The chemical potential can be calculated analytically from

$$N = \int d^3x|\psi(\mathbf{r})|^2 = \int d^3x\left(\frac{\mu}{g} - \sum_i \frac{m\omega_i^2}{2}x_i^2\right) \tag{1.31}$$

which, after working out the integral, gives the result

$$\mu(N) = \frac{\hbar\omega_{ho}}{2}\left(15N\frac{a_s}{a_{ho}}\right)^{2/5} \tag{1.32}$$

where a_{ho} and ω_{ho} are the geometric averages of the characteristic lengths and frequencies, respectively, of the harmonic potential. These are defined in the following way

$$\omega_{ho} = \sqrt[3]{\omega_x\omega_y\omega_z} \qquad a_{ho} = \sqrt{\frac{\hbar}{m\omega_{ho}}} \tag{1.33}$$

Moreover, the energy of a BEC under these conditions can be obtained easily from equation (1.19).

$$E = \int \mu(N) dN = \frac{5}{7} N \mu(N). \tag{1.34}$$

Chapter 2

Numerical Solution of the Gross-Pitaevskii equation

In this chapter we will introduce an approach useful for the numerical solution of the Gross-Pitaevskii equation (GPE). The chapter will be centred on how to write the GPE in order to ease the numerical solution.

2.1 Scaling of the Gross-Pitaevskii Equation

In general, the solution of the 3D GPE requires large memory storage and large computing times. The scaling of the GPE is used to overcome these problems by reducing the initial partial differential equation to a system of ordinary differential equations. It is done by introducing three time-dependent parameters (scaling parameters) that will absorb most of the evolution due to the time variation of the external potential. It is a method particularly well suited for condensates confined in a cigar-shaped trapping potential.

The basic scaling hypothesis for the density distribution can be stated as follows [7]

$$n(\mathbf{r},t) = \frac{1}{\prod_j \lambda_j(t)} n_0\left(\frac{r_i}{\lambda_i(t)}\right) \tag{2.1}$$

where r_i can be any coordinate x, y or z.This equation it is said to be dynamically rescaled. Inserting this hypothesis in the continuity equation (1.23), for the equality to hold we need

$$v_j(\mathbf{x},t) = \frac{\dot{\lambda}_j(t)}{\lambda_j(t)} x_j. \tag{2.2}$$

In the following we will work in the Thomas-Fermi regime and we will suppose the external potential to be a time-dependent harmonic potential whose general form in three

dimensions is

$$V(\mathbf{r},t) = \frac{1}{2}m\sum_i \omega_i^2(t) r_i^2. \tag{2.3}$$

Inserting the initial density profile for the Thomas-Fermi regime together with the scaling hypothesis in the Euler equation (1.24) we get a system of three coupled ordinary differential equations for the scaling parameters. These equations have the following form

$$\ddot{\lambda}_j(t) = \frac{\omega_j^2(0)}{\lambda_j \prod_i \lambda_i} - \omega_j^2(t)\lambda_j. \tag{2.4}$$

In order to simplify further the problem we introduce a rescaled wave function $\tilde{\psi}$ bearing in mind the above considerations. This rescaled wave function depends on the rescaled spatial coordinates $\tilde{x_i} \equiv x_i/\lambda_i(t)$ and is related to the original wave function by the following relation

$$\psi(\mathbf{r},t) = \frac{\tilde{\psi}(\{r_i/\lambda_i(t)\},t)}{\sqrt{\prod_j \lambda_j(t)}} exp\left(\frac{im}{2\hbar}\sum_j \frac{\dot{\lambda}_j(t)}{\lambda_j(t)} r_j^2\right). \tag{2.5}$$

Taking into account that we are working with an elongated condensate with cylindrical symmetry (due to the cigar-shaped potential) it is possible to factorise the rescaled wave function into an axial component $\tilde{\psi_0}(z,t)$ and a Gaussian radial component $\tilde{\phi}(x,y,t;\sigma(z,t))$ [9]. Both components will still be normalised to 1.

$$\tilde{\psi}(\mathbf{x},t) = \phi(x,y,t;\sigma(z,t))\psi_0(z,t) \tag{2.6}$$

$$\phi(x,y,t;\sigma(z,t)) = \frac{1}{\sqrt{\pi}\sigma} e^{-(x^2+y^2)/2\sigma^2} \tag{2.7}$$

At this point the 3D initial wave function has been factorise into an axial part and a radial part. Therefore, it is possible to transform the 3D GPE into an effective one-dimensional dynamically rescaled Gross-Pitaevskii equation (dr-GPE) that still describes the time evolution of the condensate. The evolution of the radial part -$\phi(x,y,t;\sigma(z,t))$- solely depends of the evolution of the parameter σ.

As stated in the previous chapter, the Gross-Pitaevskii equation can be derived from the functional $E[\psi]$ (*cf.* section 1.3.1). The evolution of both ψ_0 and σ can also be derived from that functional but, in this case, it can be further simplified. It is done through the "slowly varying approximation", in which we consider that the axial variation of the radial wave function to be negligible. Mathematically, this takes the form $\nabla^2\phi \approx \nabla_\perp^2\phi$. Integrating over the transverse coordinates (x and y), which is straightforward due to the Gaussian form of ϕ, the functional becomes [9]

$$\begin{aligned} E[\psi] \simeq \int dz \quad \psi_0^*(z) \Bigg[& \frac{\hbar^2}{2m}\frac{1}{\lambda_z^2}\nabla_z^2 - \frac{m\omega_z^2(0)z^2}{2\lambda_z\lambda_\perp^2} \\ & -\frac{\hbar^2}{2m}\frac{1}{\sigma\lambda_\perp^2} - \frac{m\omega_\perp^2(0)\sigma^2}{2\lambda_z\lambda_\perp^2} - \frac{gN}{4\pi\sigma^2}\frac{|\psi_0|^2}{\lambda_z\lambda_\perp^2}\Bigg]\psi_0(z) \end{aligned} \tag{2.8}$$

where ω_z and $\omega_\perp$ characterise the harmonic cigar shaped potential. Using the ansatz -equation (1.21)- we get the following equation for ψ_0

$$i\hbar\partial_t\psi_0 = \left\{ -\frac{\hbar^2}{2m}\frac{1}{\lambda_z^2}\nabla_z^2 + \frac{\hbar^2}{2m}\frac{1}{\sigma^2\lambda_\perp^2} + \frac{1}{\lambda_z\lambda_\perp^2}\left[\frac{m\omega_z^2(0)}{2}z^2 + \frac{m\omega_\perp^2(0)}{2}\sigma^2 + \frac{gN}{2\pi\sigma^2}|\psi_0|^2\right]\right\} \tag{2.9}$$

with

$$\sigma(z,t) = a_\perp\sqrt[4]{\lambda_z(t) + 2aN|\psi_0(z,t)|}. \tag{2.10}$$

The combination of these two equations gives a one-dimensional nonlinear Schrödinger equation for ψ_0, which is the dynamically rescaled Gross-Pitaevskii equation (dr-GPE) [9]. This equation depends on the scaling parameters whose time evolution is given by equation (2.4).

2.2 Dimensionless form of the dr-GPE

In order to solve these equations numerically it is convenient to put them in a dimensionless form. This is done by rescaling all quantities by some characteristic scale of the system, so that the new ones are dimensionless. In this case, we do it through the next set of changes

$$\tilde{t} = \omega_j t \qquad \tilde{\sigma} = \frac{\sigma}{a_\perp} \qquad \tilde{z} = \frac{z}{a_z} \qquad |\tilde{\psi_0}|^2 = \frac{|\psi_0|^2}{a_z} \tag{2.11}$$

where $a_z = \sqrt{\hbar/m\omega_z}$ and $a_\perp = \sqrt{\hbar/m\omega_\perp}$. Introducing these new variables into the dr-GPE, the equation for the width of the Gaussian and the equation of the scaling parameters we get the following set of dimensionless equations

$$i\frac{\partial\psi_0}{\partial\tilde{t}} = \left\{ -\frac{1}{2\lambda_z^2}\nabla_{\tilde{z}}{}^2 + \frac{\omega_\perp}{\omega_z}\frac{1}{2\tilde{\sigma}\lambda_\perp{}^2} + \frac{1}{\lambda_z\lambda_\perp{}^2}\left(\frac{\tilde{z}^2}{2} + \frac{\omega_\perp}{\omega_z}\frac{\tilde{\sigma}^2}{2} + \frac{\omega_\perp}{\omega_z}\frac{2aN|\tilde{\psi_0}|^2}{\tilde{\sigma}^2}\right)\right\}\psi_0 \tag{2.12}$$

$$\tilde{\sigma}(\tilde{z},\tilde{t}) = \sqrt[4]{\lambda_z(t) + 2aN|\tilde{\psi_0}|^2} \tag{2.13}$$

$$\frac{\partial^2\lambda_j(t)}{\partial\tilde{t}^2} = \frac{1}{\lambda_j\prod_i\lambda_i} - \lambda_j \tag{2.14}$$

This technique it is not only useful to solve the dr-GPE numerically, it also provides the information given by the solution of the equation in a more general form, without reference to any scale. In this sense, if what we want to study is the general properties of this equation under certain circumstances or initial parameters it will be more illustrative to give the solution in a dimensionless form. Therefore, the results given in the next chapter will be given without dimensions.

Now we are prepared to solve the GPE numerically. The scaling equation can be solved by a standard Runge-Kutta algorithm (fourth order in our case) [12]. The dr-GPE is more

complex and the Split-Step Fourier method, which is introduced in the Appendix A.2, will be helpful.

The solution of the dr-GPE gives the time evolution of the condensate but it remains to be found its initial state. The initial distribution of the BEC can be calculated using the steepest descent method (*cf.* Appendix A.1) as we assume the initial distribution is the ground state of the system. All these techniques and methods enable us to solve completely the problem of a freely expanding condensate.

Chapter 3

Interference between two BECs

We now proceed to study the case of two freely expanding cigar-shaped condensates that merge. This analysis is motivated by the landmark experiment performed in 1997 by the group led by Wolfgang Ketterle at MIT that gave experimental confirmation of the interference between two freely expanding BECs [11]. They reported matter-wave interference fringes with a period of around 15μm created by two condensates initially separated by around 40μm after a free expansion of 40ms. This demonstrated experimentally for the first time the coherence properties of Bose condensed atoms.

The result of their experiment is shown in Figure 3.1. It can be seen clearly the fringes formed by the two interfering condensates. The result of this experiment was analysed theoretically in [14] with a high degree of agreement between the experimental observation and the numerical simulation.

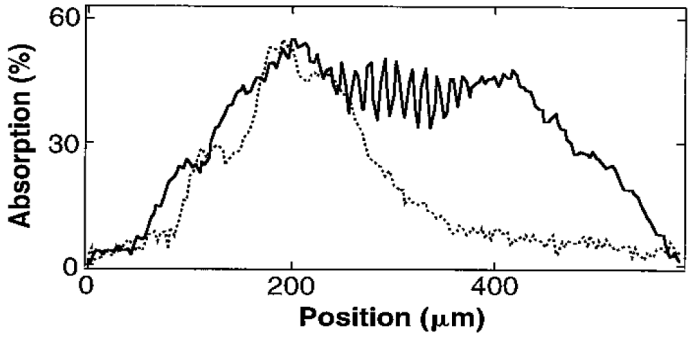

Figure 3.1: *Experimental density profile for the case of two interfering condensates (solid line) and for the case of a single condensate (dotted line). Figure obtained from reference [11].*

In the following we will perform a theoretical analysis of this phenomenon, both analytically and numerically.

3.1 Analytical study

Making use of the Gross-Pitaevskii theory developed in Chapter 1, we will demonstrate that two condensates that merge show interference phenomena. This derivation does not intend to be totally accurate, it is just a first approximation, and, therefore, we will make some simplifications such as ignoring the interaction between the two condensates.

Lets consider the initial case of two condensates (denoted by a and b) that are sufficiently separated in space to consider their overlap to be zero. Then, the order parameter that describes the system can be written in the following way

$$\psi(\mathbf{r}) = \psi_a(\mathbf{r},t) + e^{i\varphi}\psi_b(\mathbf{r},t) \tag{3.1}$$

where φ is the relative phase of the two condensates. This relative phase will play a crucial role in interference phenomena.

When the two condensates fully overlap, the density -see equation (1.4)- will have the form

$$n(\mathbf{r},t) = |\psi_a(\mathbf{r},t)|^2 + |\psi_b(\mathbf{r},t)|^2 + 2\sqrt{|\psi_a(\mathbf{r},t)||\psi_b(\mathbf{r},t)|}\cos\left(\varphi + S_b(\mathbf{r},t) - S_a(\mathbf{r},t)\right) \tag{3.2}$$

where, using the same notation as in equation (1.22), S_a and S_b are the time evolution of the phases of condensate a and condensate b respectively. It can be seen clearly that when two condensate merge interference fringes appear in their density profile due to the cosine term in equation (3.2). This is a consequence of the coherence properties of BECs.

The evolution of the phases of the condensates can be obtained by using equation (1.26) in the case of $V_{ext} = 0$ and in the Thomas-Fermi limit, that is neglecting the quantum pressure term. Then equation (1.26) becomes

$$\hbar\frac{\partial}{\partial t}S(\mathbf{r}) + \frac{1}{2}m\mathbf{v}_s^2 = 0 \tag{3.3}$$

that has as asymptotic solution for large times (see Chapter 15 of Ref. [8])

$$S(\mathbf{r}) \to \frac{1}{2}\frac{mr^2}{\hbar t} \tag{3.4}$$

It then follows that the argument in the cosine of equation (3.2) is

$$S_b(\mathbf{r},t) - S_a(\mathbf{r},t) + \varphi = \frac{md}{\hbar t}z + \varphi \tag{3.5}$$

where d is the initial distance between condensates and the condensates. Then, equation (3.2) becomes

$$n(\mathbf{r},t) = |\psi_a(\mathbf{r},t)|^2 + |\psi_b(\mathbf{r},t)|^2 + 2\sqrt{|\psi_a(\mathbf{r},t)||\psi_b(\mathbf{r},t)|}\cos\left(\frac{md}{\hbar t}z + \varphi\right). \tag{3.6}$$

This expression describes the density modulations of the two expanding condensates with fringes orthogonal to the z-axis. It predicts a spacing between two consecutive fringes of

$$\lambda = \frac{ht}{md}. \tag{3.7}$$

The position of the fringes is fixed by the initial value of the relative phase, φ, while the amplitude of the modulations will be determined by the overlapping of the two condensates as the cosine term is multiplied by $2\sqrt{|\psi_a(\mathbf{r},t)||\psi_b(\mathbf{r},t)|}$.

It is also possible to see the consequences of the coherence in momentum space. Let us consider the case of two separated identical condensates. This implies $\psi_a(\mathbf{r}) = \psi_b(\mathbf{r}+\mathbf{d})$. Then the order parameters are related, in momentum space, in the following way [8]

$$\psi_a(\mathbf{p}) = e^{-i\mathbf{p}\cdot\mathbf{d}/\hbar}\psi_b(\mathbf{r}) \tag{3.8}$$

where $\psi(\mathbf{p}) = (2\pi\hbar)^{-3/2}\int d\mathbf{r}e^{-i\mathbf{p}\cdot\mathbf{d}/\hbar}\psi(\mathbf{r})$. The previous equation explicitly shows that, even though the two condensates are separated in space, there is overlap in momentum space. Consequently, interference fringes will become visible in momentum space given by the following momentum distribution

$$n(\mathbf{p}) = |\psi_a(\mathbf{p}) + \psi_b(\mathbf{p})|^2 = 2\left[1 + \cos\left(\frac{\mathbf{p}\cdot\mathbf{d}}{\hbar}\right)\right] n_a(\mathbf{p}) \tag{3.9}$$

where $n_a(\mathbf{p}) = n_b(\mathbf{p})$ is the momentum distribution of each condensate. Equation (3.9) predicts interference fringes appearing in momentum space as equation (3.6) does in coordinate space.

As anticipated, in the derivation of this result we have ignored some effects, like the interaction between the two condensates. For a more quantitative and accurate analysis of this kind of phenomena we will solve numerically the dr-GPE discussed in the previous chapter.

3.2 Numerical study

The numerical solution of the GPE requires further details about the trapping potentials and the way the two condensates are produced. We shall start with a single condensate, trapped in a harmonic anisotropic trap with cylindrical symmetry of the form

$$V_{ho} = \frac{1}{2}m\omega_\perp^2 r_\perp^2 + \frac{1}{2}m\omega_z^2 z^2 \tag{3.10}$$

with $\omega_\perp = 2\pi\cdot 250s^{-1}$ and $\omega_z = 2\pi\cdot 19s^{-1}$ (as in Ref. [14]). Therefore, the condensate will be cigar-shaped, that is, it will have an elongated geometry aligned with the z axis.

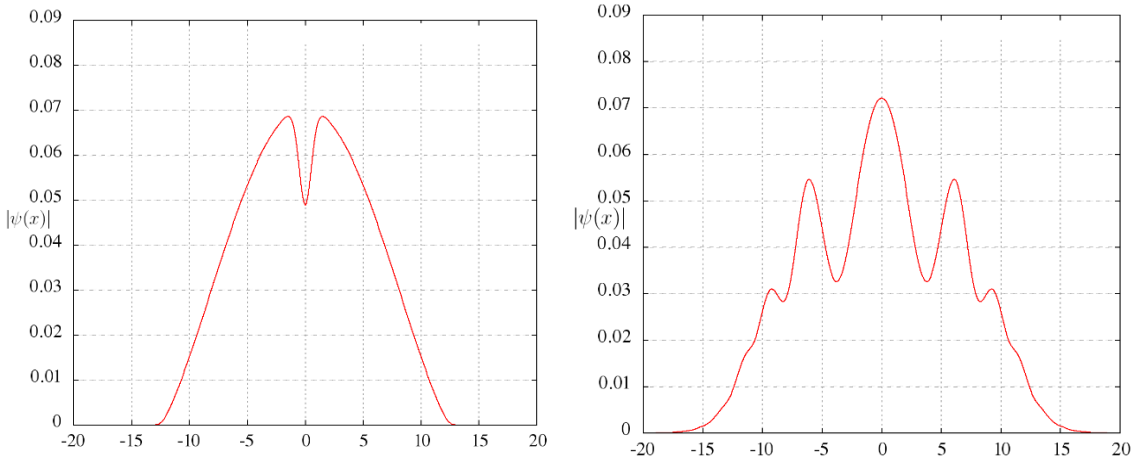

Figure 3.2: *(a) Initial ($t = 0$) and (b) final ($t = 40ms$) density distributions of the condensate for $V_0 = 10$.*

Once fixed the trapping potential it is necessary to separate the two condensates. Experimentally, it is done with a laser beam. In our simulation we will use a potential of the form

$$V_{sep} = V_0 \cdot \exp(-2z^2) \tag{3.11}$$

that simulates the potential used in Ref. [15], where V_0 is a parameter that can be varied and represents the height of the barrier that separates both condensates. Hence, we have a condensate in a harmonic trapping potential that is split up into two different parts due to the separating potential we have introduced. When both potentials are switched off the condensates will expand freely and will merge showing the interference fringes predicted above.

Having detailed the problem and using the procedures explained in the appendix we are in a position to solve the dr-GPE numerically. As mentioned before, the results given in this section will be given in a dimensionless form.

The first case of study is when $V_0 = 10$. The density pattern along the z axis for the initial distribution is shown in Figure 3.2a. As explained at the end of chapter 2, this initial distribution is calculated using the steepest descent method (*cf.* Appendix A.1) as we assume the initial distribution is the ground state of the system. It can be seen that the separation between the two condensates is not complete. Once obtained the ground state of the system the potentials are switched off and the system evolves freely for 40ms. It is usual to refer to this time of free evolution as time-of-flight. The evolution in time is obtained by solving the dr-GPE, as explained in the previous chapter, by the Split-Step Fourier Method (*cf.* Appendix A.2). The density pattern for $t = 40$ms is shown in Figure 3.2b. The central peak that dominates is a characteristic of this case that does not appear in the following one.

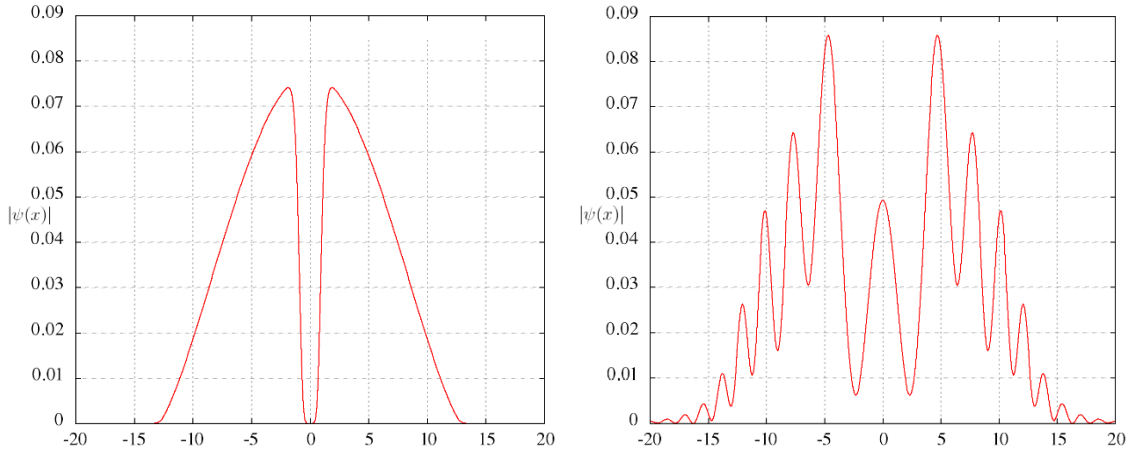

Figure 3.3: *(a) Initial ($t = 0$) and (b) final ($t = 40ms$) density distributions of the condensate for $V_0 = 100$.*

It is worth repeating this study for $V_0 = 100$. In this case, in the initial state, there is complete separation between the two condensates, a feature that will affect remarkably its evolution. Both the initial density pattern and the final one ($t = 40$ms) can be seen in Figure 3.3. In this case there is also a central peak but, in contrast with Figure 3.2b, it is smaller than the surrounding ones. This happens during all the evolution. This case is similar to the experimental one of Ref. [11], though the differences between Figure 3.1 and Figure 3.3 are due to different initial conditions. However, there is some qualitative agreement as interference fringes can be seen in both cases.

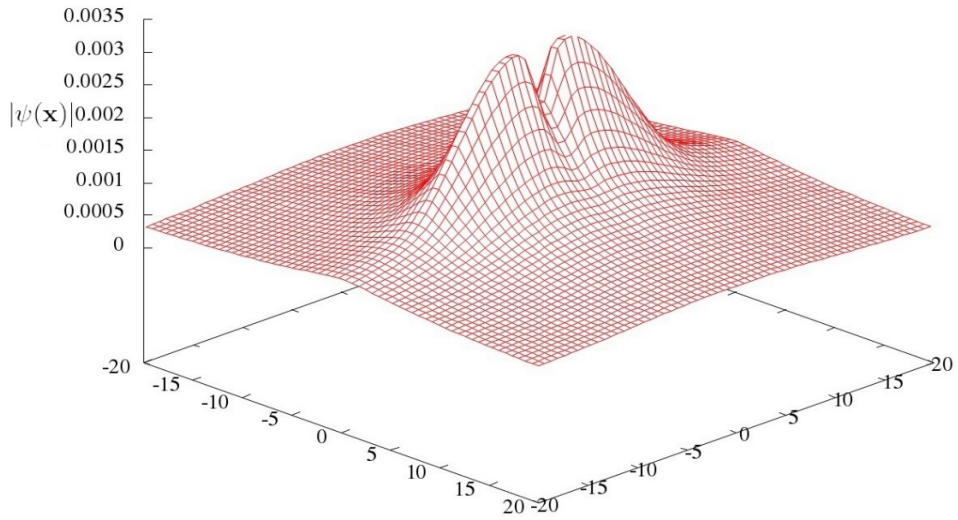

Figure 3.4: *Column density of the BEC at $t = 0$ for $V_0 = 100$.*

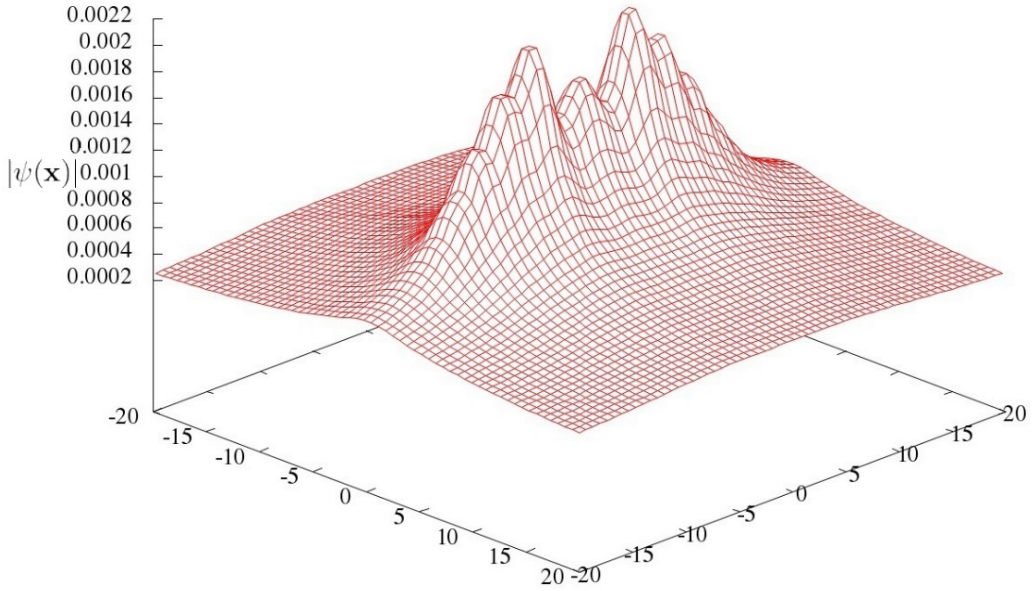

Figure 3.5: *Column density of the BEC at* $t = 40ms$ *for* $V_0 = 100$.

In the previous figures only the z axis has been shown but it is important to remember that we are dealing with a three dimensional system. In Figures 3.4 and 3.5 it is shown the density initial and final distributions in the $x - z$ plane. The y coordinate has been integrated and the result is what is called the column density, i.e. the density of the condensate in three dimensions is integrated along the y axis in Figures 3.4 and 3.5. The column density is an important quantity when making predictions as it is usually measured in experiments.

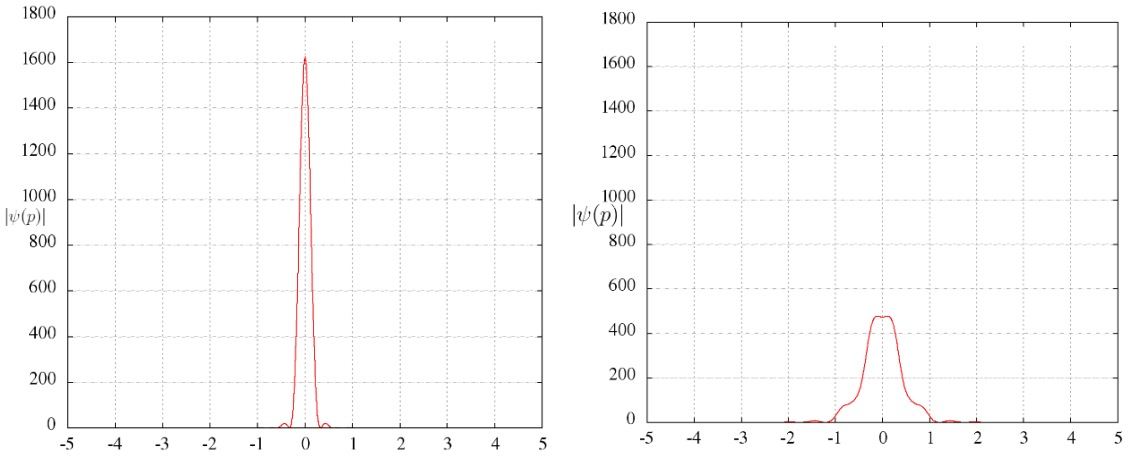

(a) (b)

Figure 3.6: *(a) Initial* ($t = 0$) *and (b) final* ($t = 40ms$) *momentum distributions of the condensate for* $V_0 = 10$.

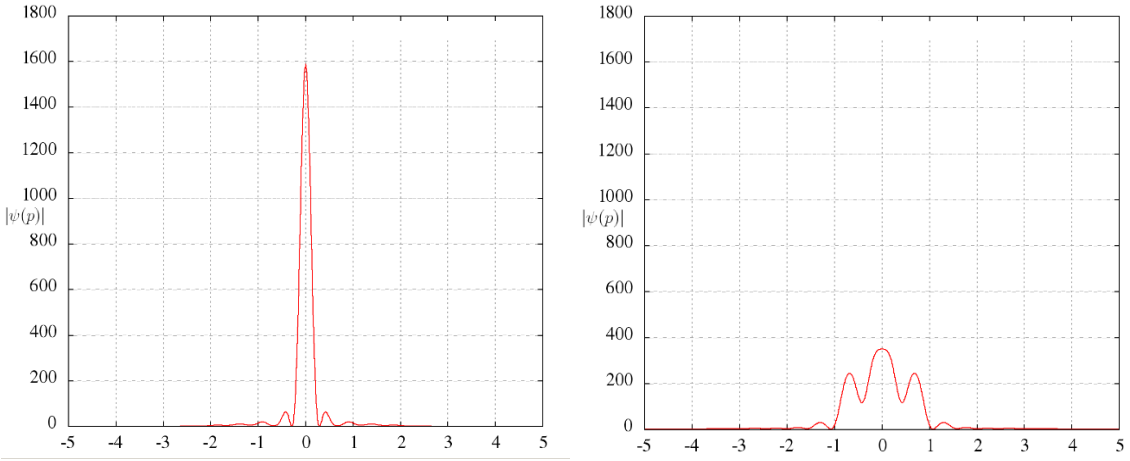

Figure 3.7: *(a) Initial ($t = 0$) and (b) final ($t = 40ms$) momentum distributions of the condensate for $V_0 = 100$.*

It is also interesting to analyse the momentum distribution of a BEC. Figures 3.6 and 3.7 show the momentum distribution of the system at the beginning (a) and at $t = 40$ms (b), for $V_0 = 10$ (Figure 3.6) and $V_0 = 100$ (Figure 3.7). In Figure 3.6 ($V_0 = 10$) the momentum distribution just shows the peak of the momentum distribution widening when the condensate is released from the trap. Figure 3.7 ($V_0 = 100$) is much more interesting as the complete separation of condensates allows us to see that also in the momentum space interference fringes form in a similar way as in the position space, phenomenon also predicted by the analytical study of the previous section.

The analytical study also predicts that the separation of the fringes will increase linearly with time (see equation (3.7)). It is interesting to see if the numerical simulation agrees with this theoretical prediction and, for this purpose, Figure 3.8 (in the next page) was obtained. In that figure the evolution with time of the average separation between two consecutive fringes is shown. Only the central fringes were taken into account as they are the more visible ones. There is some agreement with the analytical prediction as it can be easily seen that the fringes get further apart as time goes by. For large times (above 20 ms) the relation between the fringe separation and time is linear, but below this threshold the linear relation predicted by equation (3.7) no longer exits. However, we can still regard equation (3.7) as a good qualitative description of the fringe spacing for large enough times.

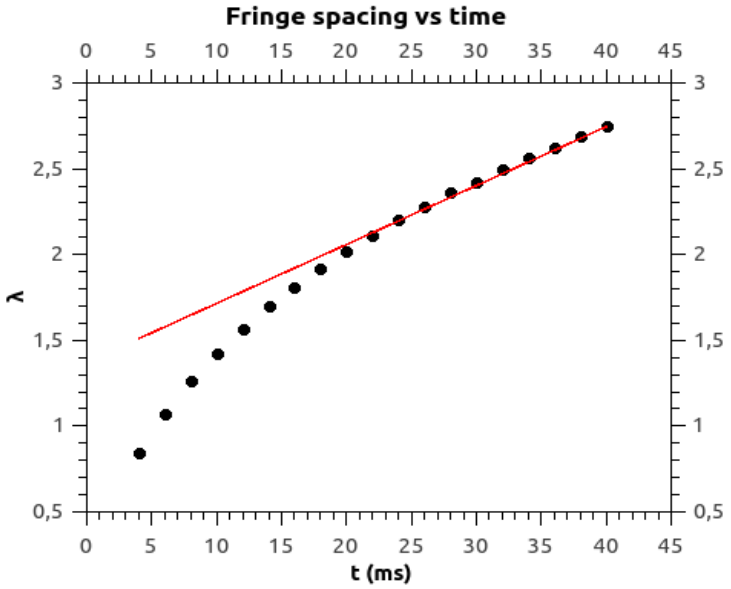

Figure 3.8: *Distance between two consecutive fringes during the evolution of the condensate for* $V_0 = 100$. *Only fringes in the central section were taken into account.*

Chapter 4

Conclusions

The aim of this dissertation was to study the interference phenomena that appear when two BECs are freely expanding and merge. For a successful description of this phenomenon we have used the Gross-Pitaevskii theory presented in chapter 1.

There have been several approaches to this task. The first one was a purely analytical one where a derivation of several properties of the evolution of a system formed by two separated BECs that expand freely was presented. The main conclusion was that a modulation in the density pattern should appear, as it does in interference phenomena. In addition, other properties of these modulations such as the linear time dependence of the separation between two consecutive fringes were predicted.

Afterwards, we obtained some numerical solutions of the GPE following the methods given in chapter 2 and in the Appendix A. We found a high level of agreement between the analytical prediction and the numerical solutions of the GPE, confirming most of the properties mentioned above, namely the appearance of interference fringes and the linear time dependence of the separation between the central fringes only for sufficiently large times (above 20ms). It is worth noticing that while in the analytical approach to the problem it was necessary to make approximations that not always were justified, in the numerical resolution, given the exact parameters of the system, enables us to make much more accurate predictions.

Finally, we have compared the numerical and analytical predictions with the experimental evidence provided by the experiment of W. Ketterle *et al.* [11]. The numerical simulation does not intend to be an exact reproduction of the experiment just a qualitative verification of the effect so there must be differences between the numerical prediction and the experimental results. However, several general properties of these kind of systems have been outlined throughout the text and this properties are common to the analytical prediction, numerical solution and experimental data. The most important of them is the

appearance of interference fringes in the evolution of this type of systems and which was predicted both analytically and numerically.

Appendix A

Numerical methods

A.1 Steepest Descent Method

In order to solve numerically the GPE it is necessary to determine the initial state of the condensate. This initial state will be obtained from the Steepest Descent method.

The method of steepest descent or gradient descent is a first-order algorithm to find a local minimum of a function. The main idea of this method is to reach the ground state of the condensate, which is the state of minimum energy, by modifying an initial wave function, ψ. In order to know how to modify conveniently our wave function we need to know the energy functional. By changing the wave function in the direction of $-\nabla E$ we assure the new wave function will be a state of less energy than the previous one.

$$\psi^{n+1} = \psi^n - d\tau \nabla E \tag{A.1}$$

This is an example of the steps it is necessary to take in order to minimise the energy of ψ where n and $n+1$ just denote the number of steps taken [12]. In equation A.1 $d\tau$ is a measure of the "length" of each step. In our case we will take as initial wave function the one dimensional wave function of the Thomas Fermi limit (given in section 1.4, equation (1.30)) in the case the external potential is an harmonic potential of frequency ω. The reason to choose this specific wave function is that we expect to be similar to the true initial state. By taking small steps in a direction opposite to the gradient (and recalculating the gradient after each step) one will eventually reach the initial state we are searching for. In addition, a condition of normalisation has to be imposed to the new wave function obtained after each step.

A.2 Split-Step Fourier Method

This method has been used to solve the dr-GPE equation discussed in this dissertation. The idea underlying this method is to divide the equation into two parts, one referring to the momentum operator and the other to the position operator.

Let us consider the evolution of a wave functions that obeys the Schrödinger equation during an infinitesimal time step dt. The evolution from t to $t + dt$ is carried out in the following way

$$\psi(x, t + dt) = e^{-idt(T+V)/\hbar}\psi(x, t) \tag{A.2}$$

where T is the kinetic energy and refers to the momentum representation and V is the potential energy and refers to the position representation. Therefore, we need to multiply ψ in the position representation by the function $e^{-idtV/\hbar}$ and by $e^{-idtT/\hbar}$ in the momentum representation, *i.e.*, after the Fourier transform $\mathcal{F}[\psi(x, t)]$. Yet, these two operators, T and V, do not commute so this splitting cannot be done directly.

Split-Step methods try to avoid this problem with the following approximation

$$e^{\lambda(A+B)} \simeq e^{\lambda\beta_n B}e^{\lambda\alpha_n A}...e^{\lambda\beta_1 B}e^{\lambda\alpha_1 A} \tag{A.3}$$

The simplest way of implementing this approximation is by choosing only three non-zero coefficients, namely, $\alpha_1 = \alpha_2 = 1/2$ and $\beta_1 = 1$ or vice versa. This combination has an error of $\mathcal{O}(\lambda^3)$.

However, the interacting term in the GPE equation makes it nonlinear so the approximation made above has to be adapted to this equation. The square of the wave function behaves like a potential energy and it could be included in the potential energy term. In order to preserve the accuracy of the method it is necessary to use always the most recent wave function available. The algorithm goes as follows [10]

$$\psi_1 = e^{\frac{idt}{4\hbar}\frac{\partial^2}{\partial x^2}}\psi(x, t) \tag{A.4}$$

$$\psi_2 = e^{-\frac{idt}{\hbar}(V(x)+g|\psi_1|^2)}\psi_1 \tag{A.5}$$

$$\psi(x, t + dt) = e^{\frac{idt}{4\hbar}\frac{\partial^2}{\partial x^2}}\psi_2. \tag{A.6}$$

Each of this parts will be computed in the appropriate representation, that is, for the first and third part, in the momentum representation; and for the second one, in the position representation.

This is the algorithm used in the program to solve the dr-GPE equation and that gives the evolution with time of the order parameter of the Bose-Einstein condensate. However, a slight modification was made in order to make the algorithm faster: the order of the

steps was inverted as follows

$$\psi_1 = e^{-\frac{idt}{2\hbar}(V(x)+g|\psi|^2)}\psi \tag{A.7}$$

$$\psi_2 = e^{\frac{idt}{2\hbar}\frac{\partial^2}{\partial x^2}}\psi_1 \tag{A.8}$$

$$\psi(x, t+dt) = e^{-\frac{idt}{2\hbar}(V(x)+g|\psi_2|^2)}\psi_2. \tag{A.9}$$

In this way it is only necessary to make the Fourier transform only once and not twice.

Therefore, the algorithm used in the program to solve the dr-GPE equation and that gives the evolution with time of the order parameter of the Bose-Einstein condensate is the second version of the split-step Fourier method.

Bibliography

[1] A. Einstein, Sitzungsberichte der Preussichen Akademie der Wissenchaften, p.261 (1924).

[2] M. H. Anderson, J. R. Ensher, M. R. Matthews, C. E. Wieman and E. A. Cornell, *Observation of Bose-Einstein Condensation in a Dilute Atomic Vapor*, Science **269**, 198 (1995).

[3] K. B. Davis, M. -O. Mewes, M. R. Andrews, N. J. van Druten, D. S. Durfee, D. M. Kurn and W. Ketterle, *Bose-Einstein Condensation in a Gas of Sodium Atoms*, Phys. Rev. Lett. **75**, 3969 (1995).

[4] C. J. Pethick and H. Smith, *Bose-Einstein condensation in dilute gases*, Cambridge University Press (2001).

[5] A. J. Leggett, *Bose-Einstein condensation in the alkali gases: Some fundamental concepts*, Rev. Mod. Phys. **73**, 307 (2001).

[6] K. F. Riley, M. P. Hobson and S. J. Bence, *Mathematical methods for Physics and engineering*, Cambridge University Press (2003).

[7] M. Modugno, *An introduction to the theory of Bose-Einstein condensation in trapped gases* (2015)

[8] L. Pitaevskii and S. Stringari, *Bose-Einstein Condensation*, Oxford Science Publications (2003).

[9] P. Massignan and M. Modugno, *One-dimensional model for the dynamics and expansion of elongated Bose-Einstein condensates*, Phys. Rev. A **67** (2003).

[10] J. Javanainen and J. Ruostekoski, *Split-step Fourier methods for the Gross-Pitaevskii equation*, arxiv.org (2004).

[11] M. R. Andrews, C. G. Townsend, H. -J. Miesner, D. S. Durfee, D. M. Kurn and W. Ketterle, *Observation of Interference Between Two Bose Condensates*, Science **275**, 637 (1997).

[12] W. H. Press, S. A. Teukolsky, W. T. Vetterling and B. P. Flannery, *Numerical Recipes in Fortran 77 The Art of Scientific Computing*, Cambridge University Press (1992).

[13] A. J. Leggett, *Broken Gauge Symmetry in a Bose Condensate*, Cambridge University Press (1995).

[14] A. Röhrl, M. Naraschewski, A. Schenzle and H. Wallis, *Transition from Phase Locking to the Interference of Independent Bose Condensates: Theory versus Experiment*, Phys. Rev. Lett. **78**, 4143 (1997).

[15] H. Wallis, A. Röhrl, M. Naraschewski and A. Schenzle, *Phase-space dynamics of Bose condensates: Interference versus interaction*, Phys. Rev. A, **55**, 2109, (1997).